Check for updates

Received: 21 December 2023 | Revised: 24 March 2024 | Accepted: 19 April 2024

DOI: 10.1111/jmi.13310

Journal of Microscopy RMS

ORIGINAL ARTICLE

Analysis of microscopy techniques to measure segregation in continuous-cast steel slabs

Araf Al Rafi[1] | **Begoña Santillana**[2] | **Renfei Feng**[3] | **Brian G. Thomas**[4] | **André B. Phillion**[1]

[1]Department of Materials Science and Engineering, McMaster University, Hamilton, Ontario, Canada

[2]Tata Steel, R&D, IJmuiden, the Netherlands

[3]Canadian Light Source, University of Saskatchewan, Saskatoon, Canada

[4]Department of Mechanical Engineering, Colorado School of Mines, Golden, Colorado, USA

Correspondence
André B. Phillion, Department of Materials Science and Engineering, McMaster University, Hamilton, Ontario, L8S 4L8, Canada.
Email: philliab@mcmaster.ca

Funding information
Natural Sciences and Engineering Research Council of Canada; McMaster Steel Research Centre

Summary

The accurate characterisation of centreline segregation requires precise measurements of composition variations over large length scales (10^{-1} m) across the centreline of the cast product, while having high resolution, sufficient to quantify the significant composition variations between dendrites due to microsegregation at very small length scales (10^{-5}m). This study investigates the potential of a novel microscopy technique, named Synchrotron Micro X-ray Flurorescence (SMXRF), to generate large-scale high-resolution segregation maps from a steel sample taken from a thin slab caster. Two methods, Point Analysis and Regression Analysis, are proposed for SMXRF data calibration. By comparing with the traditional Laser-Induced Breakdown Spectroscopy (LIBS), and Electron Probe Micro Analyser (EPMA) techniques, we show that SMXRF is successful in quantitative characterisation of centreline segregation. Over large areas (e.g. 12 × 16 mm^2) and at high resolution (10–50 μm pixel size) various techniques yield comparable outcomes in terms of composition maps and solute profiles. The findings also highlight the importance of both high spatial resolution and large field of view to have a quantitative, accurate, and efficient measurement tool to investigate segregation phenomena.

KEYWORDS
centreline segregation, continuous casting, EPMA, LIBS, SMXRF

1 | INTRODUCTION

Spatial variation in alloy composition in a casting occurs because solute is usually rejected by the advancing solidification front and enriches the liquid.[1] Microsegregation occurs within the dendritic structure of the alloy, while macrosegregation occurs at the scale of the casting when microsegregated liquid moves due to flow.[2] In the continuous casting process for steels, macrosegregation that occurs along the centreline region and across the width of the strand in the casting direction is known as centreline segregation. The occurrence of centreline segregation has a detrimental effect on the mechanical properties of the steel. Particularly, locations of high centreline segregation often act as crack initiation sites due to differences in grain structure and/or mechanical properties. In high-alloy steels, excessive centreline segregation can lead to unintentional formation of brittle martensite in the

This is an open access article under the terms of the Creative Commons Attribution License, which permits use, distribution and reproduction in any medium, provided the original work is properly cited.
© 2024 The Authors. *Journal of Microscopy* published by John Wiley & Sons Ltd on behalf of Royal Microscopical Society.

centreline during subsequent heat treatment leading to product fracture and fatigue failures in service.[3]

Solving this problem requires accurate and cost-effective measurement method(s) to quantify the degree of centreline macrosegregation. This is difficult due to the multiscale nature of the problem, which demands high-resolution measurements over a large region. Industrially, one classic practice is to use the Norme Française AFNOR (NFA) rating system,[4] which involves etching the sample with 2% Nital (2% nitric acid in iso-propanol) and evaluating the surface through a scoring chart. However, this method lacks quantifiable measurement of segregation with the results being subject to interpretation.

Another approach, referred to as 'carbon drilling', entails drilling core samples through different locations and then measuring the carbon content via standard techniques. But this method requires a significant number of drillings and has limited spatial resolution due to the time required for sample preparation.[5]

Recent decades have seen the development of new surface analysis techniques for precisely measuring macrosegregation, including energy dispersive X-ray imaging, optical emission spectroscopy, and wet chemical methods.[6] These advances in composition analysis methods have enhanced quality control procedures and provided crucial data to quantify macrosegregation, in order to improve computational models of the phenomenon, in addition to enabling feedback from plant experiments.

A good quality measurement method of macrosegregation should obtain high spatial resolution and a large field of view (FOV). The variations in dendritic microstructure cause large compositional differences across small distances, which requires high spatial resolution to detect and quantify. Statistical characterisation of the real macrosegregation distribution in a representative portion of a real commercial cast slab requires a large FOV. The development of new surface analysis methods have improved our ability to study macrosegregation, but thus far are still unable to satisfy both requirements.

One of the most popular imaging techniques to analyse broad regions is X-Ray Fluorescence (XRF) spectroscopy.[7] However, in this technique, the spatial resolution is limited. A more sophisticated form of XRF is the Micro-XRF, also known as MXRF, that analyses extremely small spots ($<20\ \mu$m) using microfocused X-ray beams. However, the scan times are long, so the FOV is restricted to small areas.

Another efficient technique is Laser-Induced Breakdown Spectroscopy (LIBS), which uses high-power laser pulses to create microplasma on the sample surface. During the cooling process, the plasma emits light with discrete spectral peaks that is used to determine the solute composition in a non-contact manner.[8] LIBS has the advantage of quick analysis and relatively high spatial resolution.[8] However, the operational parameters of the LIBS excitation source heavily depend on the environment in which it is placed.[9] For instance, the surrounding temperature can affect the plasma formation, while moisture accumulation due to high humidity can affect the lasers interaction with the sample. Moreover, LIBS is a destructive analytical method, since the formation of microplasma leads to localised sample melting or ablation.

Last but not least, Electron Probe Micro-Analysis (EPMA), which focuses a high-energy electron beam on the sample and examines the produced X-rays, also provides quantitative evaluation of solute composition with a high spatial resolution.[10] EPMA is one of the most accurate quantitative method of elemental analysis, with sensitivity at the level of ppm. However, EPMA has high capital costs, requires a lot of time to prepare samples, and has a very small FOV.

Recently, a new method has been developed on the VESPERS (**VE**ry **S**ensitive Elemental and Structural **P**robe **E**mploying **R**adiation from a **S**ynchrotron) beamline at the Canadian Light Source to efficiently assess material composition using synchrotron X-ray fluorescence spectroscopy.[11] This new method, known as Synchrotron Micro X-ray Fluorescence Spectroscopy (SMXRF), presents new opportunities for accurately and efficiently quantifying macrosegregation during continuous casting of steel with both high spatial resolution and large field of view.[11] However, SMXRF method is able to quantify composition for heavier elements, such as the Mn distribution in steel, but not for lighter elements such as Si or C, due to high attenuation from air, and the high-Fe environment.

One of the primary challenges encountered while using various microscopy techniques for elemental analysis is to calibrate the system for converting the acquired spectra into compositional data (either wt.% or at.%). In most cases, calibration is done in two steps. First, a spectrometer collects the spectra and analyses the characteristic wavelength and peaks of different elements.[12] Next, the peak intensities are analysed to calculate the element concentration using some reference standards of known composition.[12–14]. The main challenge in this methodology is the spectral overlap between elements. In the case of steels, Fe is the predominant element, and dominates the acquired spectral data. In comparison, the signal from the other elements is substantially weaker. To resolve this issue, dedicated spectrum analysis software is used to de-convolute the overlapping peaks and subtract the background to calculate the peak intensity accurately.[12] However, a significant amount of time can be required in order to capture sufficient data points to quantify the amount of minor elements.

13652818, 0, Downloaded from https://onlinelibrary.wiley.com/doi/10.1111/jmi.13310, Wiley Online Library on [28/04/2024]. See the Terms and Conditions (https://onlinelibrary.wiley.com/terms-and-conditions) on Wiley Online Library for rules of use; OA articles are governed by the applicable Creative Commons License

The SMXRF offers two distinct methods for elemental analysis: surface mapping and point analysis. SMXRF surface mapping can be used to quickly acquire qualitative data over a large field of view. With this technique the sample stage moves quickly, causing the beam to stay on each point for a very short amount of time (e.g. 0.1 s for every 10 μm). However, only the relative composition based on the ratio of the intensity peaks of various elements is obtained. SMXRF point analysis is used to make a quantitative measurement. With this technique, the beam remains at one user defined 'spot' or 'point' for a considerable amount of time (e.g. 100 s for each spot) in order to capture the spectrum with sufficient statistics to quantify mass fraction. The spot size is user defined and can be as small as 5 μm. This limits the number of points that can be examined within a reasonable amount of time. As a result, the time needed to measure a large field of view is prohibitive.

In the current study, we investigate the application of SMXRF to provide Mn composition maps of steel centreline samples with high resolution over a large field of view for better analysis of segregation. We develop two different calibration methods and examine how well the results match the results against the LIBS and EMPA techniques. Finally, we carry out a comparative analysis to understand the relative importance of spatial resolution and field of view in measuring centreline segregation in continuous-cast commercial steel.

2 | MATERIALS AND METHODS

2.1 | Steel sample used for analysis

A sample of as-cast, low-carbon, aluminum-killed steel, of 70 × 30 × 18.5 mm^3 having nominal composition that includes Fe-0.22C-2.00Mn- 1.00Si (wt.%) was provided by Tata Steel IJmuiden (Netherlands) for this analysis. The sample was taken from the central region of a sheet product that was cast at a speed of 4.5 m/min at Tata Steel's Direct Sheet Plant (DSP) thin slab caster. Figure 1 shows an image of the sample including its orientation with respect to the casting direction and the location of the fields of view that were analysed with each measurement method.

EPMA was carried out first, followed by LIBS, followed by SMXRF. Prior to conducting EPMA, the sample was prepared via standard metallographic techniques. Specifically, it was ground and then polished unembedded in a bespoke sample holder that also fit the EPMA sample holder. No sample preparation was performed between EPMA and LIBS. Because LIBS slightly damages the surface, the sample was subsequently repolished using medium-grit (1200) silica paper before the SMXRF procedure.

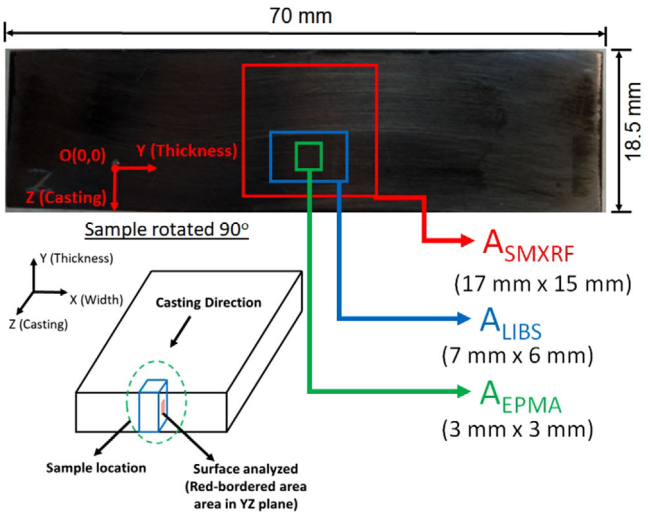

FIGURE 1 Overview of the steel sample including the sample dimensions and orientation with respect to the casting direction, the scan areas for SMXRF, LIBS and EPMA, and the origin for the point analysis.

2.2 | Characterisation methods

Three different surface analysis techniques (SMXRF, LIBS and EPMA) were employed to measure the Mn composition of the sample and to evaluate the microstructure. This element was chosen because it has a high atomic number (suitable for SMXRF) and relatively high composition, making it easier to quantify the spectral signal. Moreover, the significant influence of Mn composition on steel properties also played a vital role in making it the element of interest.

SMXRF was carried out on the VESPERS beamline at the Canadian Light Source. This beamline uses a bending magnet source to deliver a microscopic X-ray beam having a spectral range of 6–30 keV and a variable spot size. The double crystal/multilayer monochromator produces X-rays with bandwidths of 10%, 1.6% and 0.01%, which can alter the excitation condition to suit the analytical condition. For the current analysis, a 1.6% bandpass beam was used for the measurements. Data are acquired via a Vortex® silicon drift detector for XRF and a Pilatus® 1M pixel area detector for XRD. Figure 2 shows a schematic of the locations of the XRF and XRD detectors surrounding the sample, inside the secondary optical enclosure. The sample stage is positioned 90° from the incoming beam, and the detector 45°, so the sample surface is perpendicular to the beam. The sample stage has a travel range of 40 mm in vertical, and 150 mm in horizontal, defining a FOV of 40 mm × 150 mm. Figure 2 also shows the location of a pair of bendable Kirkpatrick-Baez (KB) mirror system for controlling beam focus. A more detailed discussion

13652818, 0, Downloaded from https://onlinelibrary.wiley.com/doi/10.1111/jmi.13310, Wiley Online Library on [28/04/2024]. See the Terms and Conditions (https://onlinelibrary.wiley.com/terms-and-conditions) on Wiley Online Library for rules of use; OA articles are governed by the applicable Creative Commons License

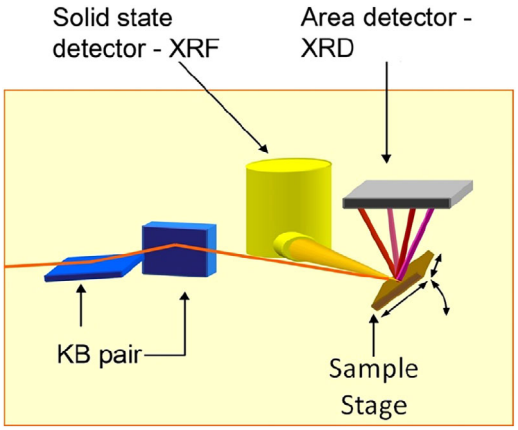

FIGURE 2 Schematic of the SMXRF showing the XRF and XRD detectors as well as the Kirkpatrick-Baez mirror system.[11].

regarding the SMXRF instrumentation can be found in the literature.[11]

The LIBS analysis was conducted using a SPECTRAL[15,16] desktop analyser. This instrument is capable of automated scanning with 100 μm resolution for topographical and elemental mapping. The utilisation of a high-power laser and an echelle spectrometer enables excitation and analysis of a wide range of elements with high spatial resolution. The broadband gated LIBS improves the signal-to-noise ratio to enhance the detection of light elements. The pulsed laser utilised in the analysis features a repetition rate of 20 Hz and a pulse energy of 120 mJ.

The EPMA analysis was conducted at Tata Steel IJmuiden in The Netherlands. A tungsten filament served as the primary electron beam source, supplemented by magnetic lenses to focus and guide the beam effectively. The beam has an accelerating voltage range of 15–30 kV, allowing a balance between spatial resolution and the depth of X-ray generation. The beam current has a wide range, from a few picoamperes (pA) to several nanoamperes (nA), to meet specific requirements. Detection of the X-ray beam was achieved using a Wavelength-Dispersive X-ray Spectrometer (WDS) crystal detector. For mapping or line scanning, preinstalled software is used to automate the sequence by specifying the count time per point. To mitigate potential carbon (C) contamination, an oxygen jet was employed during the analysis.

A brief description of LIBS and EPMA has been provided in the literature review, above. Further details on these two techniques can be found in Refs. (8, 10, 15, 17).

2.3 | Data acquisition – surface mapping

Mn composition area maps were acquired using the three techniques for the FOVs shown in Figure 1. The large FOV for SMXRF Surface Mapping (A_{SMXRF} = 255 mm^2) was made possible by high-speed synchrotron imaging. The FOV for LIBS (A_{LIBS} = 42 mm^2) and EMPA (A_{EPMA} = 9 mm^2) were smaller owing to technique limitations. As can be seen, areas A_{LIBS} and A_{EPMA} fall within A_{SMXRF} and as close to the centreline as possible. This allowed for direct comparison for the measured Mn content between the different measurements.

The data were acquired as follows. First, for SMXRF surface mapping, data were collected using a spot size of 5 μm with a pixel pitch of 50 μm, and a dwell time of 100 ms per spot. To avoid the dominated XRF signal from Fe and to increase the sensitivity to detecting Mn, the energy of the incoming X-rays was tuned to 7 keV which is below Fe K-edge. Second, for LIBS, data were collected using a laser energy of 3 mJ, with a spot size and pixel pitch of 100 μm in an Ar environment. Third, for EPMA, data were collected using a pixel spot size and pixel pitch of 10 μm and a dwell time of 1 s for both the peak and background. The operating conditions for EPMA were an accelerating voltage of 15 kV and a beam current of 200 nA, with an oxygen jet utilised to minimise carbon contamination. These last conditions were chosen to balance the spatial resolution, acquisition time, and FOV.

In terms of scan duration, the SMXRF scan was 8 h to analyse a 255 mm^2 area with a pixel size of 50 μm, the LIBS scan was 3 h to analyse the 42 mm^2 area with a pixel size of 100 μm, and the EPMA scan was about 1 week for 9 mm^2 area with a pixel size of 10 μm.

2.3.1 | Data acquisition – point analysis

SMXRF point analysis was performed on the sample in order to directly measure the Mn content in wt.%. In total, 100 points were systematically analysed in a grid format (10 rows and 10 columns) with a step size of 1 mm and spot size of 5 μm. The large step size was used to cover a large surface area. The corresponding values in arbitrary unit (a.u.) were also extracted from these same 100 locations. Figure 3 shows an example case to illustrate the difference between surface mapping and point analysis. Specifically, surface mapping was conducted on each orange square, while point analysis was conducted on each purple circle. Please note that this example shows point analysis with only 8 points, and not the 100 points actually acquired.

2.4 | Data calibration

Calibration is necessary in order to convert the measured peak intensities to weight percentages. For both LIBS and EPMA, standard instrument calibration methods were used in this work to quantify the measured

13652818, 0, Downloaded from https://onlinelibrary.wiley.com/doi/10.1111/jmi.13310, Wiley Online Library on [28/04/2024]. See the Terms and Conditions (https://onlinelibrary.wiley.com/terms-and-conditions) on Wiley Online Library for rules of use; OA articles are governed by the applicable Creative Commons License

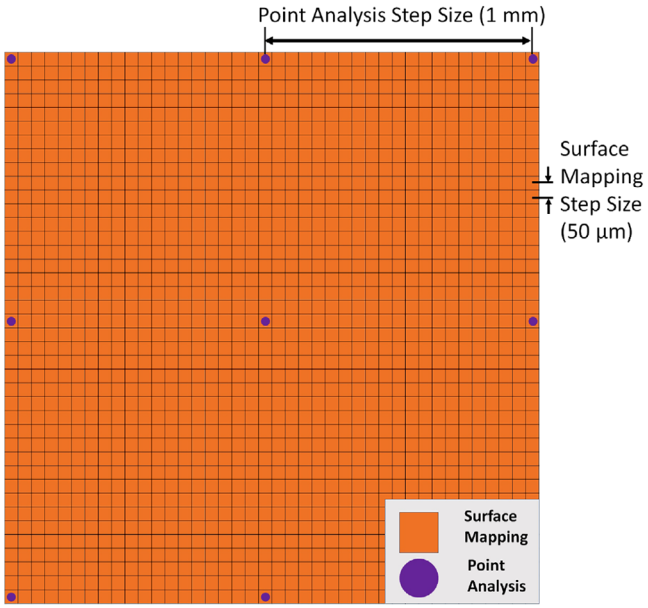

FIGURE 3 Example case of data acquisition using SMXRF for a 3 × 3 grid. The surface mapping has a step size of 50 μm and the point analysis has a spot size of 5 μm and step size of 1 mm. Note that this drawing is for illustration only; the study actually used a 10 × 10 grid format over a 100 mm^2 area.

composition.[8,18] However, there is not yet an established calibration procedure to quantify the SMXRF data into accurate composition measurements for large field of view composition maps. In Section 4, two distinct calibration methods are proposed to quantify the SMXRF data.

3 | COMPOSITION DATA MAPS

The SMXRF, LIBS, and EPMA data have been analysed to understand the Mn distribution and quantify macrosegregation. All the data were handled using in-house R software. They were organised as an X × Y (= N) matrix where X and Y represent the number of rows and columns, respectively, and N represents the total number of data points or pixels.

Figure 4 displays the Mn composition maps obtained using three different techniques. The SMXRF image represents the relative Mn composition (ratio of Mn intensity to the incoming flux intensity) referred as arbitrary unit (a.u.), while the LIBS and EPMA images are depicted in weight percent (wt.%). These composition maps provide insights into the distribution of Mn in the centreline and far-field regions of the sample.

The centreline segregation is evident in all images, characterised by isolated and interconnected Mn-rich pools along the centreline. The dendritic structures are observed as Mn-poor regions, whereas the interdendritic regions are seen as Mn-rich areas. In the far-field region, numerous high-intensity pixels of Mn suggest the presence of nonmetallic inclusions rich in Mn.

The SMXRF image also displays the formation of three distinct segregation bands. A positive centreline segregation band with an average width of 2 mm is visible along the centreline. Next to the centreline segregation band, there are two other bands that are comparatively low in Mn. These banded structures are also visible, to some degree, in the LIBS image. However, they are not present in the EPMA image due to its small field of view. Having the large field of view enabled by SMXRF enables the capture of a fulsome view of the negative segregation band. A closer inspection of the SMXRF image (A_{SMXRF}) also reveals solute enrichment along the grain boundaries, which can be used to estimate the shape and size of the original δ-ferrite grains.

4 | METHODS TO CALIBRATE SMXRF DATA

Two different methods have been developed to transform the SMXRF data in a.u. shown in Figure 4 into quantitative surface mapping(rapidly scanned) composition measurements.

The first method to calibrate SMXRF is named Point Analysis Method. This method transforms the raw data from SMXRF surface mapping into quantitative compositions using the 100 measurements obtained from the SMXRF point analysis data acquisition. A simple averaging of the data is performed for this calibration,

$$Mn^{ij}_{wt\%} = \frac{Mn^{avg}_{wt\%}}{Mn^{avg}_{a.u.}} \times Mn^{ij}_{a.u.}, \quad (1)$$

where $Mn^{avg}_{a.u.}$ is the average Mn content of the raw data from SMXRF surface mapping in a.u., $Mn^{avg}_{wt.\%}$ is the average Mn content of the one hundred measurements from SMXRF point analysis in wt.%, and Mn^{ij} is the measured (a.u.) and calibrated (wt.%) compositions with i and j being the rows and columns of the spatial coordinates.

The second method to calibrate SMXRF is named Regression Analysis Method. This method uses the calibrated LIBS measurements to calibrate the SMXRF data, by fitting a linear relationship between the two. This is made possible by assuming that the higher relative values of the SMXRF Surface Mapping data occur at the same spatial locations as the corresponding higher LIBS measurements. The method is as follows. First, the raw SMXRF Surface Mapping data in a.u. is downsampled to correspond to the LIBS data's resolution in the same area, A_{LIBS}. This is needed because the LIBS data set has a structure

13652818, 0, Downloaded from https://onlinelibrary.wiley.com/doi/10.1111/jmi.13310, Wiley Online Library on [28/04/2024]. See the Terms and Conditions (https://onlinelibrary.wiley.com/terms-and-conditions) on Wiley Online Library for rules of use; OA articles are governed by the applicable Creative Commons License

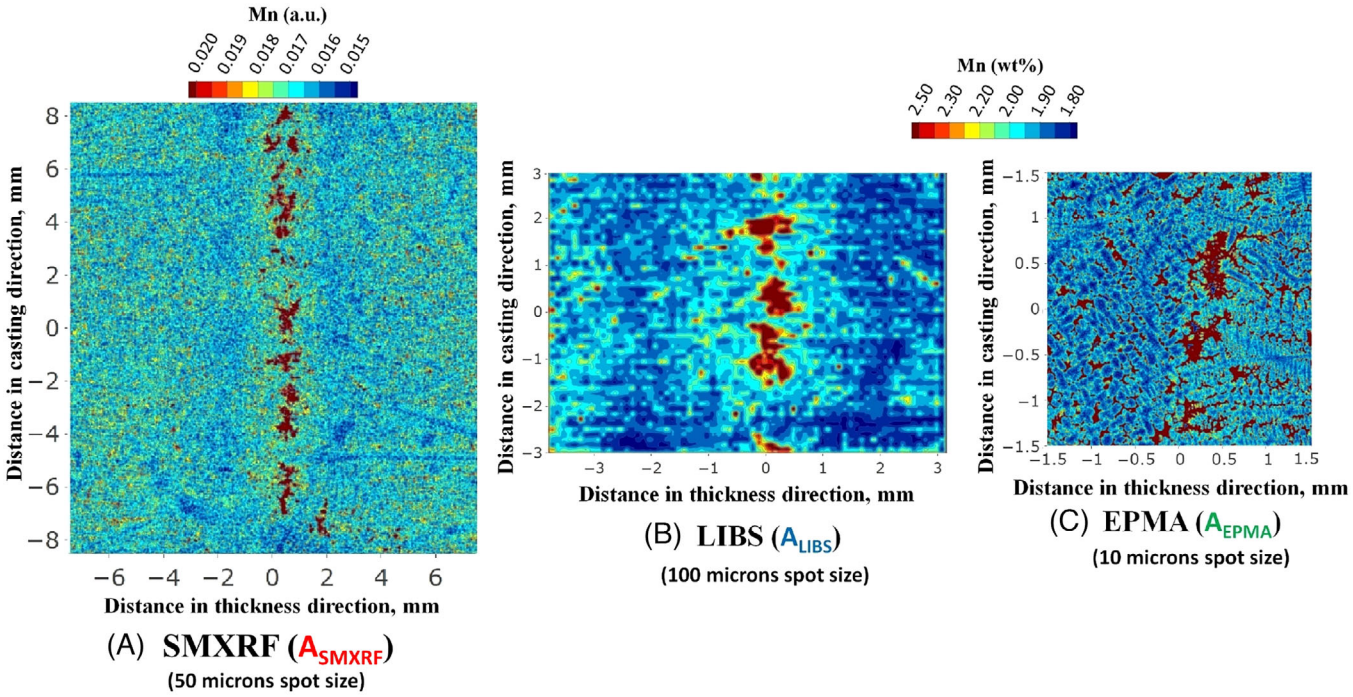

FIGURE 4 Visualisation of Mn composition maps obtained using three different microscopy techniques: SMXRF Surface Mapping, LIBS and EPMA, with corresponding spot size given in brackets. The SMXRF data are provided in a.u., whereas the calibrated LIBS and EPMA data are provided in wt.%.

of 70×60 pixels with a pixel pitch of 100 μm, while the corresponding SMXRF data set has a structure of 140×120 pixels with a pixel pitch of 50 μm. Therefore, four SMXRF data points corresponded to each LIBS data point. The downsampling was performed by taking the average of the corresponding four data points. Second, the downsampled SMXRF surface mapping data and the LIBS data were sorted were in ascending order from smallest value to large. Third, the points from each data set were paired one to one. Finally, linear regression analysis was performed to determine the best fit line.

Figure 5 shows the results of both calibration methods, the SMXRF surface mapping data correlated to the 100 point analysis measurements via the spatial coordinates (red crosses), and the SMXRF surface mapping data correlated to the LIBS measurements via sorting from smallest to largest value (black crosses). The SMXRF surface mapping data (in a.u.) is plotted on the *x*-axis, while the SMXRF point analysis data and the LIBS data (in wt.% unit) are plotted on the *y*-axis. The two calibration lines (red and black dotted lines) are also plotted, along with the equations resulting from the calibration.

As can be seen from Figure 5, both correlations are somewhat nonlinear. The first calibration method shows that the SMXRF point analysis measurements (in wt.% units) has a linear trend with the SMXRF mapping data (in a.u.) until about 2.30 wt.% Mn. However, after 2.30 wt.%, it starts to increase exponentially. This could be attributed

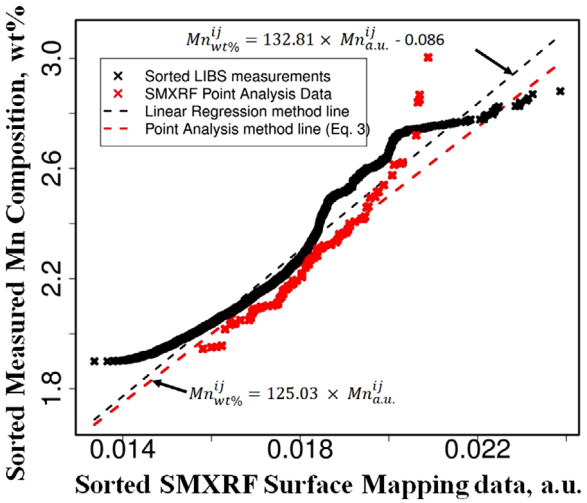

FIGURE 5 Scatter plot of Mn composition for the A_{LIBS} area, derived from Laser-Induced Breakdown Spectroscopy (LIBS) data, and its corresponding downsampled SMXRF data.

to the presence of surface contamination. The second calibration methods shows that the LIBS data has a wavy trend with the SMXRF mapping data, overestimating in some areas but underestimating in others. Since SMXRF and LIBS are two distinct microscopy techniques, with totally different working principles, the observed differences could be related to the operating conditions. For example, the material response to the laser pulse during

13652818, 0, Downloaded from https://onlinelibrary.wiley.com/doi/10.1111/jmi.13310, Wiley Online Library on [28/04/2024]. See the Terms and Conditions (https://onlinelibrary.wiley.com/terms-and-conditions) on Wiley Online Library for rules of use; OA articles are governed by the applicable Creative Commons License

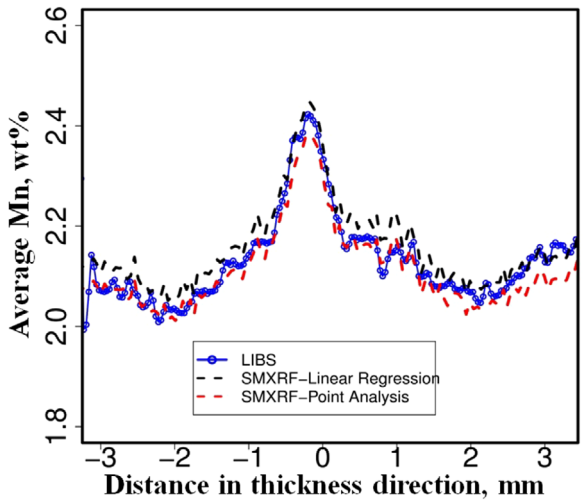

FIGURE 6 Comparison of SMXRF calibration methods with LIBS data using average Mn profile of area A_{LIBS}.

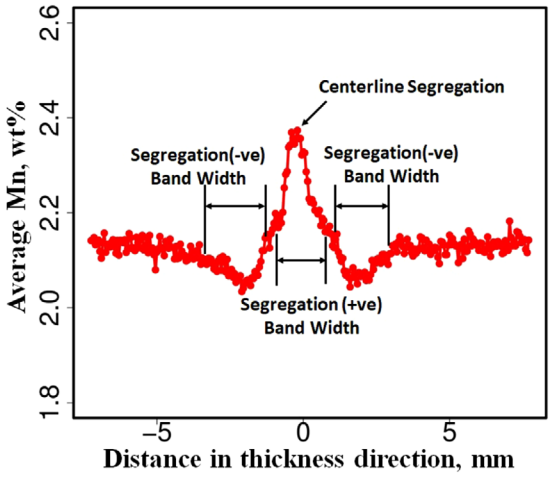

FIGURE 7 Variation of average Mn profile of A_{SMXRF} in the thickness direction (data averaged in the casting direction).

LIBS is nonlinear. Comparing the two best fit lines, it is clearly seen that calibration line from the Regression Analysis Method has a slightly larger slope than that from the Point Analysis Method. However, the negative intercept of this calibration line counteracts the effect of the larger slope.

The performance of the two calibration methods is evaluated in Figure 6 which plots the average Mn profile of the calibrated SMXRF data across the slab centreline compared with the average macrosegregation profile of the LIBS measurements. Both profiles are plotted using the data within area A_{LIBS}. For area A_{LIBS}, SMXRF has a data structure of 120×140 pixels (y and z directions). To plot the average Mn profile, the data were reduced from 120×140 2D map to 1×140 profile by averaging the data in the casting direction (z direction) and then plotting as a function of distance in the thickness direction (y direction). Similarly, the LIBS data structure for A_{LIBS} was converted from 60×70 to 1×70.

As can be seen, there is strong agreement between the calibrated SMXRF results and the LIBS measurements. The Regression Analysis calibration is seen to slightly overestimate the Mn composition. The higher composition predicted by this calibration method can be attributed to the nonlinearity existing between the downsampled SMXRF and LIBS data in Figure 5. The Point Analysis calibration shows excellent agreement with the LIBS measurements for lower composition values while slightly underestimating the high composition values at the centreline peak. Overall, both calibration methods perform equally well. They both exhibit a similar location and magnitude of the centreline segregation peak and the surrounding CET zones.

5 | RESULTS AND DISCUSSION

The calibration methods enable us to utilise SMXRF to obtain large-scale quantitative composition maps with high resolution in reasonably short times, in order to understand the solute distribution and its microscale fluctuations in the centreline and the far-field regions. For this purpose, the calibrated SMXRF data (using the Point Analysis Method) are used to plot the average Mn profile for the larger area, A_{SMXRF} in Figure 7. The figure clearly shows a pronounced peak of 2.40 wt.% at the centre, corresponding to the red centreline segregation region in Figure 4. It is evident that the extent of segregation is significant and much higher than the nominal 2.00 wt.%Mn composition. Usually, such a high degree of segregation is attributed to a cast structure having fully columnar grains.[5]

The Mn composition maps and the average solute profile can be used to evaluate the centreline segregation and the results here are consistent with a classic formation mechanism. Figures 4 and 7 both show three segregation bands at the central region. The Mn-depleted bands just next to the centreline segregation band correspond to the columnar-to-equiaxed transition (CET) whereby the growth pattern changes from columnar to equiaxed as a result of equiaxed grain nucleation taking place in the liquid likely ahead of the columnar dendritic tips.[19] The lower average composition in this zone is due to having more equiaxed grains, which comprise mainly low-alloy solid crystals likely formed higher in the caster and transported or separated from the enriched interdendritic liquid, which later accumulates in the centre region.

The zone of equiaxed grains in proximity to the centreline region serves as an indicator of the degree of centreline segregation. Usually a narrow equiaxed zone, very close to the centreline region, results in a higher degree of

13652818, 0, Downloaded from https://onlinelibrary.wiley.com/doi/10.1111/jmi.13310, Wiley Online Library on [28/04/2024]. See the Terms and Conditions (https://onlinelibrary.wiley.com/terms-and-conditions) on Wiley Online Library for rules of use; OA articles are governed by the applicable Creative Commons License

centreline segregation. The length and the severity of segregation of this zone depend on the superheat of the liquid steel.[20] High in the mould region, dendrite arms can be melted away from the solidification front and swept away by the liquid to act as little seed crystals. When superheat is low, these seeds may survive and eventually accumulate ahead of the columnar solidification front thus stopping columnar growth while also perhaps causing even more equiaxed grains to nucleate.

On the other hand, high superheat results in a narrow equiaxed zone since the majority of the seed crystals melt. High casting speed, narrow cast sections and steel with richer chemistry are often cast with higher superheat.[5] The current high-speed thin slab caster satisfies all conditions for a small equiaxed zone and wider columnar zone. This could explain why the Mn composition of the centreline region of the thin slab caster is almost 20% higher than the nominal composition.

5.1 | Comparative analysis

The measurements taken in area A_{EPMA} are used to compare the composition measurements of the three different microscopy methods investigated in this study: EPMA, LIBS and SMXRF calibrated via the Point Analysis Method. To facilitate a fair comparison, the EPMA data were downsampled to 50 and 100 μm resolutions, while the SMXRF data were also downsampled to 100 μm resolution. Figure 8 compares the Mn composition maps obtained from all 3 methods and displayed with three different spatial resolutions. The original maps are shown in Figure 8A, C and F while the downsampled images are shown in Figure 8B, D and E with grey border. The corresponding data structures of all the images are shown in a table at the top right.

At the same resolution of 100 μm in Figure 8D, E and F, the three techniques correspond well with each other, both in qualitative appearance, trends, etc., and in colours (indicating quantitative match). Note slight differences due to repolishing in between measurements, which reveals slight differences in width (x) direction.

Figure 8A, B and D showcases how the spatial resolution can affect the segregation morphology. For the highest resolution of 10 μm, the dendritic structures can be clearly seen in Figure 8A. And also in the 50 μm resolution, we can also see the dendrites and the interdendritic regions, especially if at a larger field of view (that reveals more of the microstructure, e.g. Figure 4A). The solute rejection between each pair of dendrites causes the small-scale composition variations. At the lowest resolution, Figure 8D, E and F, overall trends are visible but the dendritic details are missing. An averaging method is needed to quantify the degree of centreline segregation at this resolution.

The high-resolution images come at a cost of longer analysis time. As mentioned before, the EPMA measurement time for the 3 mm × 3 mm area seen in Figure 8A (300 × 300 data points, resolution of 10 μm) took 1 week corresponding to about 7 s per data point. For the same area, the LIBS analysis, Figure 8C (30 × 30 data points, resolution of 100 μm), required only 30 min or 2 s per data point, while the SMXRF analysis, Figure 8F (60 × 60 data points, resolution of 50 μm), required only 6 min or 0.1 s per data point! Of course, to be quantitative, SMXRF also requires a one-time calibration, which takes ~3 h with Point Analysis. Please note that SMXRF technique can also provide 10 μm resolution matching EPMA but with a much shorter analysis time. It is estimated that SMXRF would require about 3 h to measure 300 × 300 data points at a 10 μm resolution. The resolution of 50 μm was selected for SMXRF in this study since the main motivation of this study was to analyse a large field of view to obtain large scale macrosegregation maps.

Figure 9 compares the variation of Mn content in the thickness direction for a single line of data along the centreline of Figure 8A, C and F. The Mn profiles from SMXRF and LIBS match very well, but there are significant fluctuations in the EPMA data. This can be attributed to the significantly larger detail in composition variation that exists with a 10 μm resolution. The EPMA map in Figures 8A captures the real variations between dendrites, due to solute rejection from the dendrite core to the adjacent interdendritic liquid between dendrites. These individual dendrites can be barely discerned in the composition map if examined closely. While various statistical techniques have been suggested to reduce this statistical detail/noise,[21] plotting the average Mn profile and not a single line of data can provide a smoother curve while still revealing new insight into centreline segregation.

Figure 10 shows the average Mn profile for the data in Figure 8A, C and F. The data for all three images were averaged in the casting direction and plotted as a function of distance in the thickness direction, similar to the construction of Figure 6. Again, there is good agreement among the three techniques, with all three curves showing similar solute intensity at the centreline region. However, for EPMA, the location of the peak is seen to be shifted slightly to the right and shows more variability. This is due to the higher resolution of the data, and the slight variation in composition distribution (also seen between Figure 8D, E and F) caused by polishing the surface between measurements.

13652818, 0, Downloaded from https://onlinelibrary.wiley.com/doi/10.1111/jmi.13310, Wiley Online Library on [28/04/2024]. See the Terms and Conditions (https://onlinelibrary.wiley.com/terms-and-conditions) on Wiley Online Library for rules of use; OA articles are governed by the applicable Creative Commons License

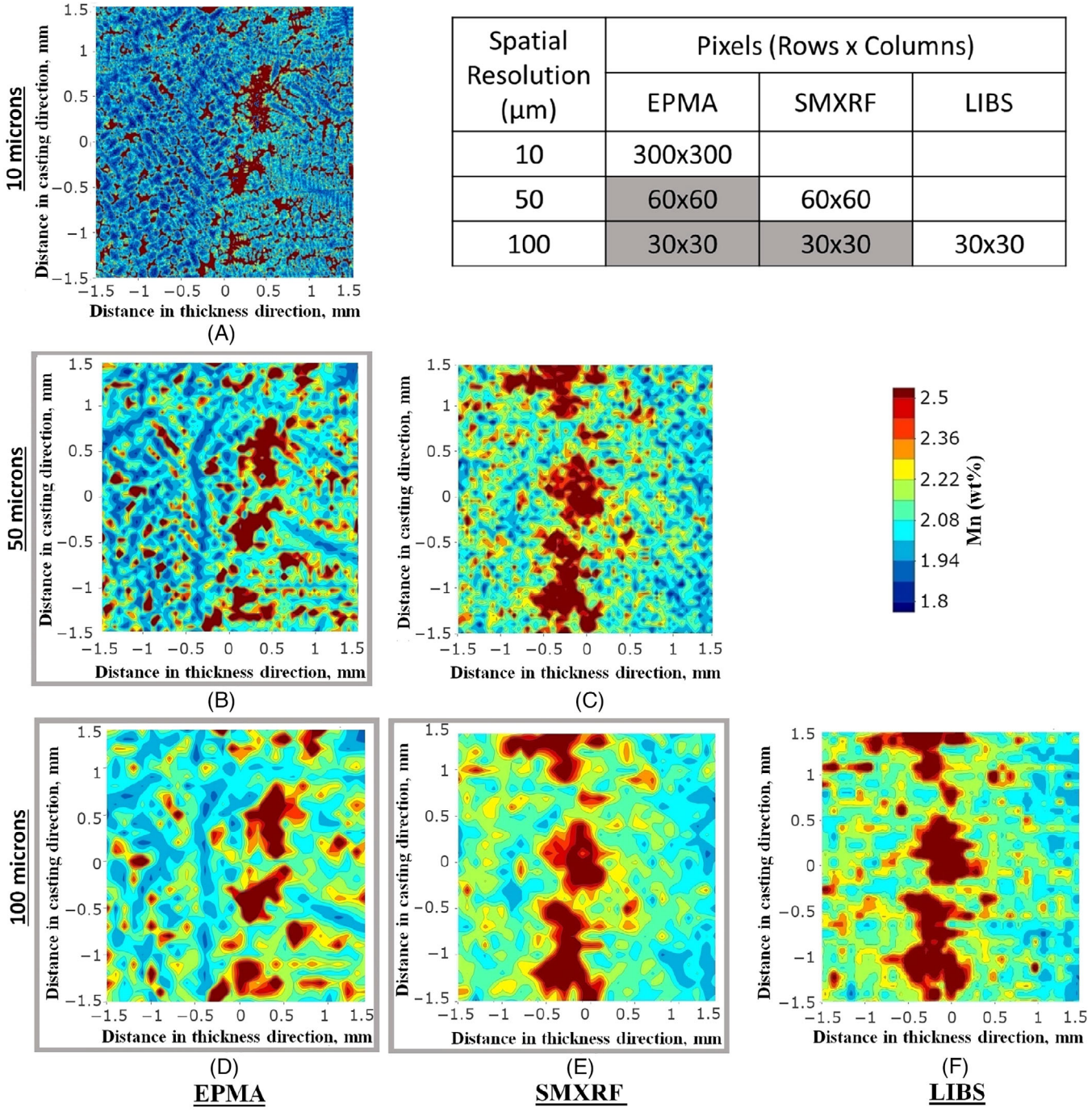

Spatial Resolution (μm)	Pixels (Rows x Columns)		
	EPMA	SMXRF	LIBS
10	300x300		
50	60x60	60x60	
100	30x30	30x30	30x30

FIGURE 8 Mn composition map of area A_{EPMA} (3 mm × 3 mm) obtained from different microscopy techniques and corresponding downsampled images.

5.2 | Statistical analysis

Figure 11 presents a more comprehensive statistical analysis of the data in Figure 8A, C and F, elucidating the amplitude of deviation from the mean composition across the three distinct techniques. The solid lines shown in Figure 8A, B, and C correspond to the mean (μ) Mn profiles previously illustrated in Figure 10. The upper dashed line and the lower dotted line signifies the values at two standard deviations away from the mean ($\mu + 2\sigma$ and $\mu - 2\sigma$) observed for each column. As can be seen in the set of figures, SMXRF and LIBS show similar levels of fluctuation, indicating that both techniques have similar type of data distribution, whereas EPMA shows rapid and more pronounced fluctuations. On one hand, this is a result of the smaller spot size in EMPA that allows for exact quantification of the Mn composition in the interdendritic regions and not the blurring that results when having a

13652818, 0, Downloaded from https://onlinelibrary.wiley.com/doi/10.1111/jmi.13310, Wiley Online Library on [28/04/2024]. See the Terms and Conditions (https://onlinelibrary.wiley.com/terms-and-conditions) on Wiley Online Library for rules of use; OA articles are governed by the applicable Creative Commons License

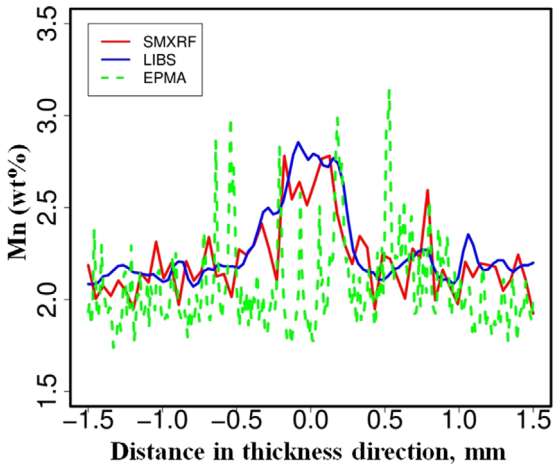

FIGURE 9 Variation of Mn content of area A_{EPMA} for a single line data in the thickness direction (along the centreline of Figure 8A, C and F).

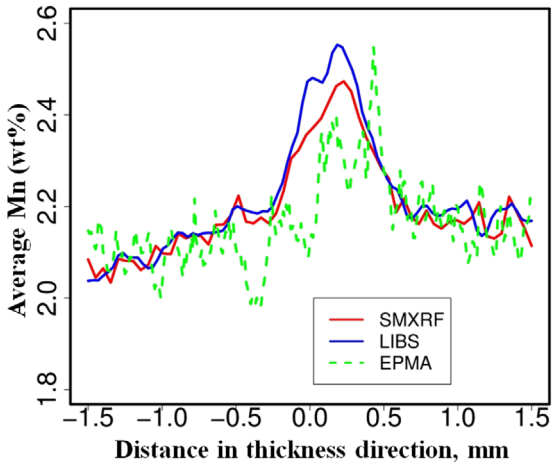

FIGURE 10 Variation of average Mn content of area A_{EPMA} in the thickness direction (averaged in casting direction) from different experimental techniques.

larger spot size in the SMXRF and LIBS analyses. On the other hand, these rapid fluctuations hint at the possible influence of external factors such as surface contamination and nonhomogeneous entities on EPMA measurement.

5.3 | Methodology comparison

The high sensitivity of SMXRF surface mapping allows for rapid data acquisition, with each point analysed in just 0.1 s. In contrast, EPMA and LIBS may take from several seconds to minutes per point. The heightened photon flux derived from highly intense and precisely collimated X-ray beams in SMXRF enhances sensitivity and expedites data collection compared to conventional X-ray sources. The stability of the synchrotron beamline further enables higher spatial resolution. Moreover, SMXRF is entirely non-destructive, contrasting with LIBS, where microplasma formation can induce local material surface melting. EPMA is also a nondestructive technique, in the context of metal alloy analysis.

Although SMXRF provides a powerful and versatile approach to fast, large-field, and high-resolution

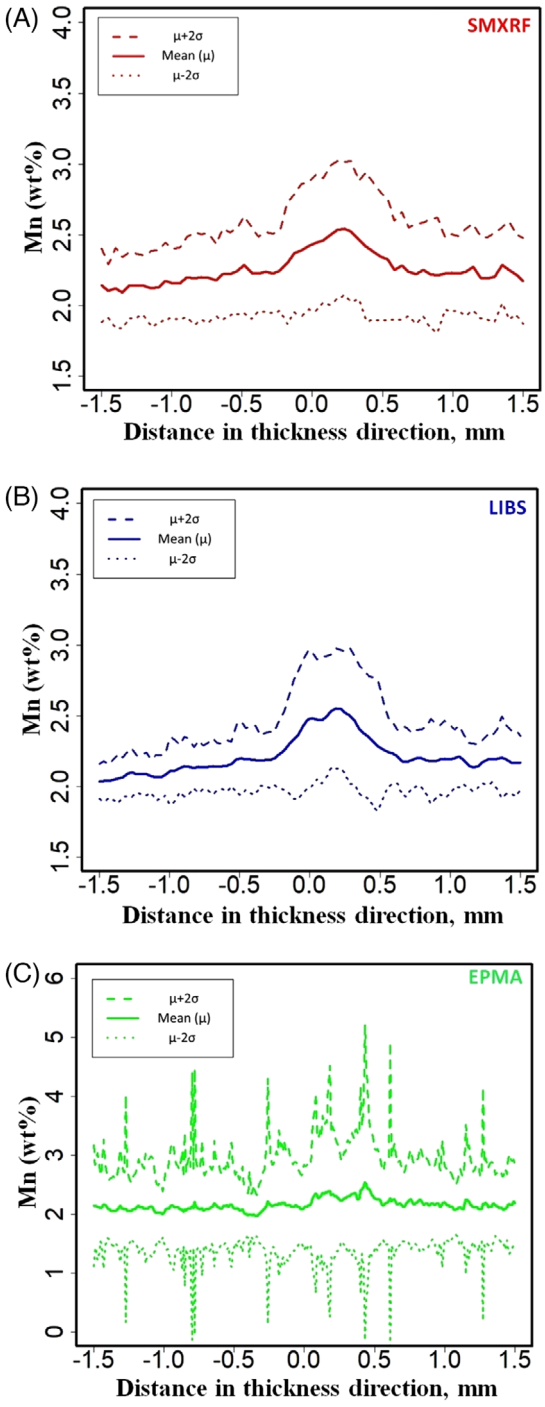

FIGURE 11 Deviation of Mn composition from the mean value in casting direction of area A_{EPMA} for (A) SMXRF, (B) LIBS and (C) EPMA.

13652818, 0, Downloaded from https://onlinelibrary.wiley.com/doi/10.1111/jmi.13310, Wiley Online Library on [28/04/2024]. See the Terms and Conditions (https://onlinelibrary.wiley.com/terms-and-conditions) on Wiley Online Library for rules of use; OA articles are governed by the applicable Creative Commons License

compositional analysis, it faces limitations in terms of beamtime availability at synchrotron facilities, making it more suitable for research and development purposes rather than industrial applications. In contrast, EPMA and LIBS offer more accessible alternatives. EPMA is regarded as the most accurate and precise technique for compositional analysis. Apart from its high spatial resolution, EPMA also has the advantage of depth profiling. By varying the energy of the electron beam, EPMA can be utilised to analyse different layers of the sample.[22] On the other hand, many LIBS instruments are portable and can be used for onsite analysis without needing sample preparation. This makes LIBS one of the best candidates for industrial compositional analysis to improve the quality control process during steel casting.[8]

The advantage of SMXRF is in achieving both large field of view and high resolution. Thus, it will provide much-needed data for validating modern continuous casting process models that are able to provide composition predictions down to the micron scale. Having the large field of view is also important for understanding variations that occur along the casting length. As is shown clearly in Figure 8, centreline segregation is not a single value at the centreline but spatially varies to a significant degree.

6 | CONCLUSIONS

In this study, a new synchrotron-based X-ray fluorescence imaging technique named SMXRF has been used to investigate centreline segregation of Mn in a continuous-cast thin slab of alloy steel. The raw data from surface mapping SMXRF are calibrated to quantitative composition maps using either of two new calibration methods. The resulting segregation maps are compared with conventional LIBS and EPMA techniques. The advantage of SMXRF over these other techniques is the combination of a large field of view and high spatial resolution, acquired in a relatively short amount of time.

Both the Point Analysis and Regression Analysis methods are able to calibrate the arbitrary units of the raw SMXRF surface maps into quantitative composition maps in weight percentage. The Point Analysis Method seems to be quite accurate for points close to the nominal composition, while the Regression Analysis Method may show improved accuracy for values far away from the nominal composition.

Composition maps using the three spectroscopy techniques are compared in the same field of view at different spatial resolutions. To enable fair comparisons at the same resolution, the data were downsampled by local averaging for the EPMA and SMXRF techniques. At the same resolution, all three techniques produced similar results.

This work shows that SMXRF is a highly efficient method to obtain large-scale composition maps with high spatial resolution with very high speed per unit area analysed. Such a combination of large field of view with high resolution is needed to investigate centreline segregation phenomena in continuously cast steels whereby the composition can vary significantly as a function of cast length. If access can be gained to synchrotron beamtime for this advanced microscopy method, SMXRF analysis can reveal the dendritic structures and grain shapes associated with centreline macrosegregation, including the negative segregation bands perhaps associated with the columnar-to-equiaxed transition. Although EPMA can provide images with even greater detail, acquiring the data requires extremely long analysis time. This effectively limits the field of view EPMA causing it to fail in capturing industrially important variations in composition. LIBS also can provide images with good detail, but its combination of resolution, field of view and acquisition time are not as detailed as EPMA, nor covering as large a field of view as SMXRF.

ACKNOWLEDGEMENTS

AR and AP gratefully acknowledge the financial support provided by the Natural Science and Engineering Research Council of Canada (NSERC) and the McMaster Steel Research Centre, along with contributions from its partner companies. BT acknowledges the Continuous Casting Center at the Colorado School of Mines. We also extend our appreciation to Tata Steel IJmuiden, the Netherlands, for providing the steel sample and conducting the EPMA analysis. The LIBS analysis was carried out by Spectral Industries within a collaboration agreement with Tata Steel R&D. We also thank the Canadian Light Source for allocating beamtime (Project – 35G12273~Phillion) to conduct SMXRF analysis on the sample for this project.

ORCID

Brian G. Thomas https://orcid.org/0000-0001-8485-3438

REFERENCES

1. Flemings, M. C., & Nereo, G. E. (1967). Macrosegregation part I. *Transactions of the Metallurgical Society of AIME*, *239*, 1449–1461.
2. Rappaz, M., & Dantzig, J. A. (2009). *Solidification*. EPFL Press.
3. Lesoult, G. (2005). Macrosegregation in steel strands and ingots: Characterisation, formation and consequences. *Materials Science and Engineering A*, *413–414*, 19–29.
4. Boué-Bigne, F. (2014). Simultaneous characterization of elemental segregation and cementite networks in high carbon steel products by spatially-resolved laser-induced breakdown spectroscopy. *Spectrochimica Acta Part B*, *96*, 21–32.
5. Choudhary, S. K., Ganguly, S., Sengupta, A., & Sharma, V. (2017). Solidification morphology and segregation in continuously cast

13652818, 0, Downloaded from https://onlinelibrary.wiley.com/doi/10.1111/jmi.13310, Wiley Online Library on [28/04/2024]. See the Terms and Conditions (https://onlinelibrary.wiley.com/terms-and-conditions) on Wiley Online Library for rules of use; OA articles are governed by the applicable Creative Commons License

steelslab. *Journal of Materials Processing Technology*, *243*, 312–321.
6. Pickering, E. J., & Holland, M. (2014). Detection of macrosegregation in a large metallic specimen using XRF. *X-Ray Spectrometry*, *41*, 493–499.
7. Potts, P. J., & Webb, P. C. (1992). X-ray fluorescence spectrometry. *Journal of Geochemical Exploration*, *44*, 251–296.
8. Boué-Bigne, F. (2008). Laser-induced breakdown spectroscopy applications in the steel industry: Rapid analysis of segregation and decarburization. *Spectrochimica Acta Part B*, *63*, 1122–1129.
9. Cremers, D. A., & Chinni, R. C. (2009). Laser-induced breakdown spectroscopy-capabilities and limitations. *Applied Spectroscopy Reviews*, *44*, 457–506.
10. Koshikawa, T., Bellet, M., Gandin, C. A., Yamamura, H., & Bobadilla, M. (2017). Experimental study and two-phase numerical modeling of macrosegregation induced by solid deformation during punch pressing of solidifying steel ingots. *Acta Materialia*, *124*, 513–527.
11. Feng, R., Gerson, A., Ice, G., Reininger, R., Yates, B., & McIntyre, S. (2007). Vespers: A beamline for combined XRF and XRD measurements. *AIP Conference Proceedings*, *879*, 872.
12. Al-Eshaikh, M. A., & Kadachi, A. (2011). Elemental analysis of steel products using x-ray fluorescence (XRF) technique. *Engineering Sciences*, *23*, 75–79.
13. Yan, C., Ju, X., Meng, Y., & Shi, X. (2019). Quantification of manganese dendritic segregation in 380CL steel billet by electron probe microanalysis. *SN Applied Science*, *1*, 623.
14. Yaguang, M., Yuxin, C., Shusen, C., Zhongqi, H., Lianbo, G., Xiangyou, L., & Xiaoyan, Z. (2018). Simultaneous analysis of Si, Mn and Ti segregation in pig iron by laser-induced breakdown spectroscopy. *Infrared and Laser Engineering*, *47*(8), 806003–0806003.
15. Spectral Industries. Laser-induced breakdown spectroscopy (LIBS). Retrieved from https://spectralindustries.com/
16. Van Den Berg, F., Santillana, B., & Hechu, K. (2022). Laser-induced breakdown spectroscopy (LIBS). European Patent Office Application 21164212.9–1020.
17. Khater, M. A. (2013). Laser-induced breakdown spectroscopy for light elements detection in steel: State of the art. *Spectrochimica Acta Part B*, *81*, 1–10.
18. Reed, S. (1993). *Electron microprobe analysis* (2nd ed.). Cambridge University Press, Cambridge.
19. Kurz, W., Bezençon, C., & Gäumann, M. (2001). Columnar to equiaxed transition in solidification processing. *Science and Technology of Advanced Materials*, *2*, 185–191.
20. Ohno, A. (1987). *Solidification: The separation theory and its practical applications*. Springer-Verlag, Berlin.
21. Gungor, M. (1989). A statistically significant experimental technique for investigating microsegregation in cast alloys. *Metallurgical and Materials Transactions*, *20A*, 2529–2533.
22. Karduck, P., & von Richthofen, A. (1995). EPMA sputter depth profiling: A new technique for quantitative in-depth analysis of layered structures. *Microscopy Microanalysis Microstructures*, *6*, 421–432.

How to cite this article: Al Rafi, A., Santillana, B., Feng, R., Thomas, B. G., & Phillion, A. B. (2024). Analysis of microscopy techniques to measure segregation in continuous-cast steel slabs. *Journal of Microscopy*, 1–12. https://doi.org/10.1111/jmi.13310

13652818, 0, Downloaded from https://onlinelibrary.wiley.com/doi/10.1111/jmi.13310, Wiley Online Library on [28/04/2024]. See the Terms and Conditions (https://onlinelibrary.wiley.com/terms-and-conditions) on Wiley Online Library for rules of use; OA articles are governed by the applicable Creative Commons License